Imaging P-wave scatterer distribution in the focal area of the 1995 M7.2 Hyogo-ken Nanbu (Kobe) Earthquake

GEOPHYSICAL RESEARCH LETTERS, VOL. 25, NO. 9, PAGES 1439-1442, MAY 1, 1998

Imaging P-wave scatterer distribution in the focal area of the 1995 M7.2 Hyogo-ken Nanbu (Kobe) Earthquake

Satoshi Matsumoto
Mining College, Akita University, Akita, Japan

Kazushige Obara
National Research Institute for Earth Science and Disaster Prevention, Tsukuba, Japan

Akira Hasegawa
Faculty of Science, Tohoku University, Sendai, Japan

Abstract. Spatial distribution of P-wave scatterers in and around the focal area of the 1995 Hyogo-ken Nanbu Earthquake (M7.2) has been estimated by using dense seismic array data. Waveforms of 12 explosions were analyzed in a frequency band of 6-10Hz range. It is difficult to estimate the inhomogeneous structure in this wavelength range from the ordinary travel time tomography, in spite of its importance for understanding earthquake-generating process. Observed waveforms were slant stacked into various directions from the array and then AGC and diffraction curve summation are applied in order to image scatterer distribution. Spatial distribution of scattering strength thus imaged shows that higher strengths are distributed beneath the hypocenter, the initiation point of the mainshock rupture, and in the southwestern part of the fault plane of the event.

Introduction

In seismograms of natural earthquakes and artificial explosions, many phases appear after arrivals of direct P and S waves. These phases can be interpreted as scattered waves by inhomogeneities distributing within the crust. Recently, *Nishigami* [1991] and *Revenaugh* [1995] estimated scatterer distributions from large amplitude phases in the coda part observed by seismic networks with station separations of several km. If we analyze seismograms recorded by small aperture array with station separations of several tens meters, ray direction approaching to the array would be determined in more detail. In the present study, we try to detect these phases and to estimate an inhomogeneous structure around the fault area of the 1995 Hyogo-ken Nanbu Earthquake.

The M7.2 Hyogo-ken Nanbu (Kobe) Earthquake that occurred in the western part of Honshu, Japan on January 17 (JST), 1995 caused severe damages in Kobe and adjacent cities and more than 6300 people were killed. Aftershock activity of this event was observed and monitored by a dense temporary seismic network [e.g., *Hirata et al.*, 1996]. Source process of this event has been studied in detail by many researchers based on observation data of seismic and GPS networks [e.g., *Ide et al.*; 1996, *Kakehi et al.*; 1996, *Yoshida et al.*; 1996]. 3-D seismic velocity structure in the focal area has been estimated by *Zhao et al.* [1996], and they discussed the relation between the obtained inhomogeneous structure and the main shock rupture. However, inhomogeneous structure in a wavelength ranges shorter than a few km has not been studied well. It is important for understanding the process of earthquake occurrence to know more detailed spatial distribution of inhomogeneity in the crust.

Paper number 98GL01090.
0094-8534/98/98GL-01090$05.00

Observation and Data

In order to detect scattered waves generated by inhomogeneities in the target area, we carried out a seismic array observation in the northern part of Awaji Island for the period from Sep. 15 to Dec. 14, 1995. The location of the array is close to the initiation point of the rupture of the Hyogo-ken Nanbu Earthquake, and is shown in Fig. 1. The array is composed of 2Hz vertical component seismometers and 1Hz 3-component seismometers with a site spacing of either 10m or 20m. 3-component seismometers were installed at 15 sites. Total numbers of observation sites and channels of this array are 162 and 192, respectively. In the present observation, seismometers are distributed two-dimensionally in order to detect scattered waves coming from various directions. Seismic signals are collected through CDP cables and recorded by two digital recorders. The recorder each having 96 channels is equipped with a sigma-delta A/D converter with 24 bit resolution. Recording time for each event is set to 60 sec with a sampling frequency of 500Hz. Earthquakes are detected automatically by taking ratios of short-term to long term average amplitudes at several sites. Waveform data from explosions, carried out by Research Group of Explosion Seismology [*R. G. E. S.*, 1996], are obtained by manual triggering.

In the present study, we analyze waveform data from 12 explosions whose locations are shown in Fig. 1. 150 - 700kg of dynamites were exploded in boreholes at these shot points. An example of record section for shot S4, the nearest shot from the array among 12 explosions, is shown in Fig.2. The waveform data are band-pass filtered in a frequency range between 6 to 10Hz with a decay of -12db/Oct. Then the coda part is amplified by AGC processing with a window length of 4 seconds. In Fig. 2, several phases are clearly recognized in the lapse time of 8 to 14 secs after direct P wave onset. These phases can be identified even in the record section without

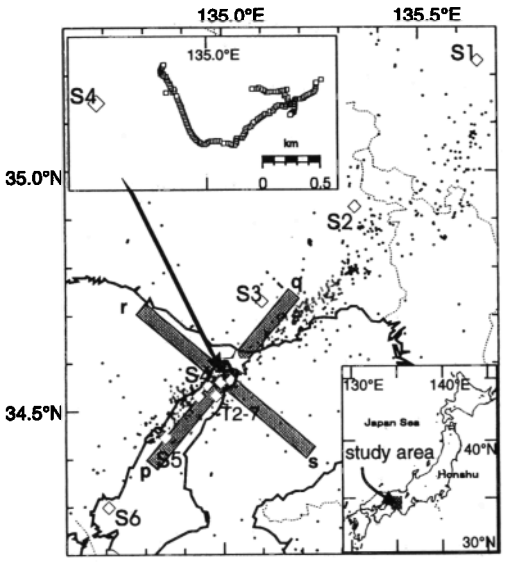

Figure 1. Map showing locations of a seismic array and explosions by R.G.E.S [*R.G.E.S*, 1996]. Open diamonds with two-letter code (S1-S6 and T2-T7) show shot points. Open squares denote locations of observation sites of the array. Hypocenters of aftershocks determined by *Hirata et al.* [1996] are shown by dots. The hypocenter of the 1995 Hyogo-ken Nanbu Earthquake is indicated by an open star. Shaded lines with p-q and r-s show the locations of vertical cross-sections shown in Fig. 6.

AGC amplitude recovery processing. In the following section, array analysis is applied to these data to estimate a detailed spatial distribution of reflectors or scatterers.

Analysis

Ray directions of scattered waves can be determined as a function of slowness and azimuth from the array. However, most of the events analyzed here have large offset distances of

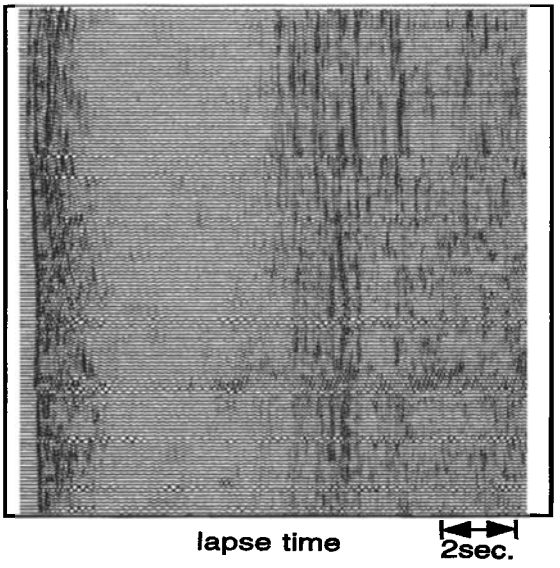

Figure 2. An example of seismic section recorded by the seismic array for shot S4. Band-pass filter of 6-10Hz and AGC processing are applied.

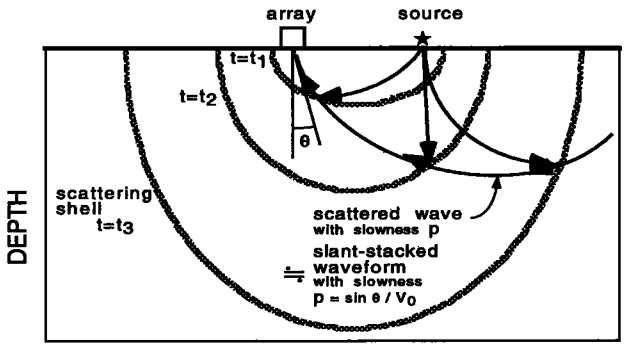

Figure 3. Schematic illustration showing relationship between slant stacking and scatterer distribution.

more than 10 km. In such a case, we cannot apply high-resolution analyses developed in exploration seismology such as CDP stacking and migration processing. Here, we propose a processing sequence to estimate spatial distribution of scattering strength as follows.

We apply slant stack processing to the observed array data to estimate scatterer distribution beneath Awaji Island. A slant stacked waveform in a certain azimuth and slowness can be regarded as scattered waves coming from that direction along the ray path with that slowness, as schematically shown in Fig. 3. In this process, waveform data in space-time domain A(x, y, t) are converted to slowness, azimuth-time domain A(p, ϕ, t). The observed waveforms are band-pass filtered (6-10Hz) and stacked in variable slownesses with azimuths of 50 and 140 degree, which are directions of parallel and perpendicular to the fault plane of the Hyogo-ken Nanbu Earthquake. The slownesses used here are from -0.18 to 0.18 with a step interval of 0.01. Time axis at each site is shifted by the static correction time to remove the effect of shallow subsurface structure. For each shot, we obtain a time difference at each site by subtracting the manually picked time from the calculated time of direct P wave arrival which is determined from the optimum wave front of that shot. After taking average the time differences of all shots, we obtain the static correction factor at each site. We assume here that scattered waves approach to the array as plane waves. Curvature of wave front of scattered waves affects the amplitude of slant stacked waveform if the time difference between spherical wave front and plane wave front at the edge of the array is greater than a quarter period for the target frequency. Therefore, we will discuss scatterers locating 1 km or more away from the array.

A slant-stacked waveform is independent of the array configuration apparently. The waveform for each shot and slowness is passed through AGC-filter with 4 seconds window length to recover amplitude in coda part. The amplitude recovery corresponds to normalizations for source energy and for scattering of energy by uniformly distributing scatterers. After slant stacking and AGC processing, the waveform is transformed again to the horizontal distance, azimuth-depth domain A(s, ϕ, z). Based on the velocity structure of the crust, s- and z-coordinates of scattered waves approaching the array can be calculated from slowness, lapse time and both locations of the hypocenter and the array. Here, we adopt a depth dependent velocity model expressed by $v(z) = v_0+kz$, where v_0 and k are 5.5 and 0.067, respectively. This velocity structure is obtained by smoothing and interpolating

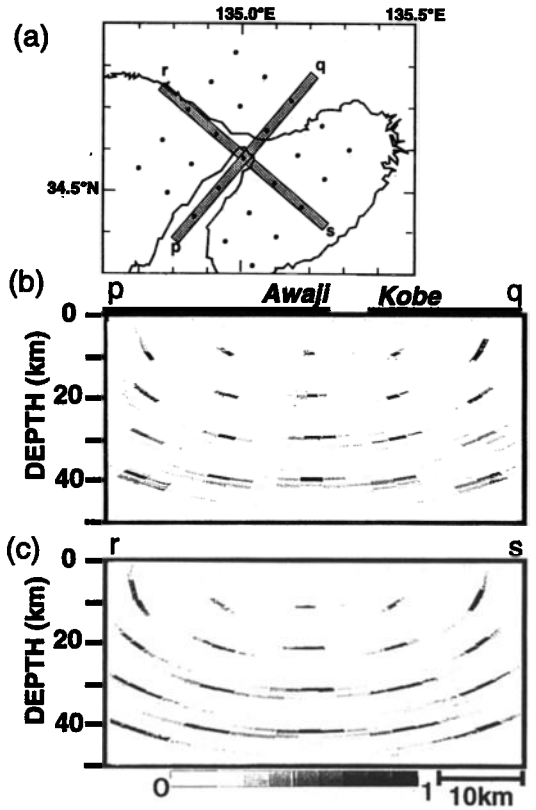

Figure 4. Resolution check by using three dimensionally distributed scatterers. (a) Map view of the locations of given scatterers. 25 x4 point scatterers are set at depths of 10, 20, 30 and 40km. (b) and (c) are vertical cross-sections of estimated scatterer distribution along the lines p-q and r-s in (a) by the processing, respectively. Estimated relative scattering strength is shown by the black and white scale at the bottom.

the four-layered model, which is adopted by Hirata et al. [1996] to determine hypocenters in this region. We also assume that multiple-scattered waves can be neglected and that the effect of mode-converted waves from P to S waves is small on vertical component seismograms analyzed here. The above process by using one event data gives a spatial distribution of scattering strength for P wave.

We stacked all the waveforms obtained from the 12 shots to improve the image of the scattering strength distribution. Although the time interval of each sample in slant stacked waveforms of events with a certain slowness is identical with each other, which is the inverse of sampling frequency of A/D converter, the distance interval corresponding each sample varies from event to event due to the transformation to $A(s, \phi, z)$ from $A(p, \phi, t)$. Especially, the sample interval of slant stacked waveforms expands in smaller lapse times. This means that waveform shape is deformed by the processing. This effect depends on the offset distance between the array and the source. Thus, directly stacking the processed waveforms of all the events would not improve S/N ratio. Therefore, we deal with the processed waveforms as energy density series $E(s, \phi, z)$ by taking power of amplitude $A(s, \phi, z)$. $E(s, \phi, z)$ with a uniform distance interval is obtained from an interpolation of $E(s, \phi, z)$ with a varying distance interval. Then we can stack them for all the shots which gives an image of spatial distribution of scattering strength for P wave.

In the present study, scattering strength is evaluated by energy density stacking. Background scattered energy clouds an image of stronger scatterer distribution as the number of stacking increases. Therefore, we subtract average density E_{av} of each energy density sequence $E(s, \phi, z)$ from $E(s, \phi, z)$ before stacking.

The processing described above is essentially identical with diffraction curve summation of energy density sequence among events. To check resolution of this method, we synthesize scattered waves from 100 point-scatterers located beneath the array for 12 events. The scatterers are uniformly distributed in a volume of 40km x40km x40km with an interval of 10km (Fig. 4). Stacked $Es(s, \phi, z)$ is obtained after the transformation from the synthesized waveform $A(x, y, t)$ to $E(s, \phi, z)$. As a result, $E(s, \phi, z)$ for a single source spreads over ten kilometers from the given location of each scatterer. However, after stacking all the events, the scatterers can be imaged correctly, and estimation error is less than a few kilometers in the shallower part as can be seen in Fig. 4.

For the homogeneous velocity model, *Sato* [1977] analytically obtained that energy density of coda wave is in proportion to scattering coefficient (g_0) based on the single isotropic scattering assumption. Therefore, ratio of energy density to smoothed coda energy envelope at a lapse time is equal to that of scattering coefficient (g) to background scattering coefficient (g_0) in the volume contributing to coda energy at that lapse time. For the depth dependent velocity structure, it can be considered that the ratio is still g/g_0. Then, we interpret that the ratio of the finally obtained $Es(s, \phi, z)$ to E_{av} is the ratio $(g-g_0)/g_0$.

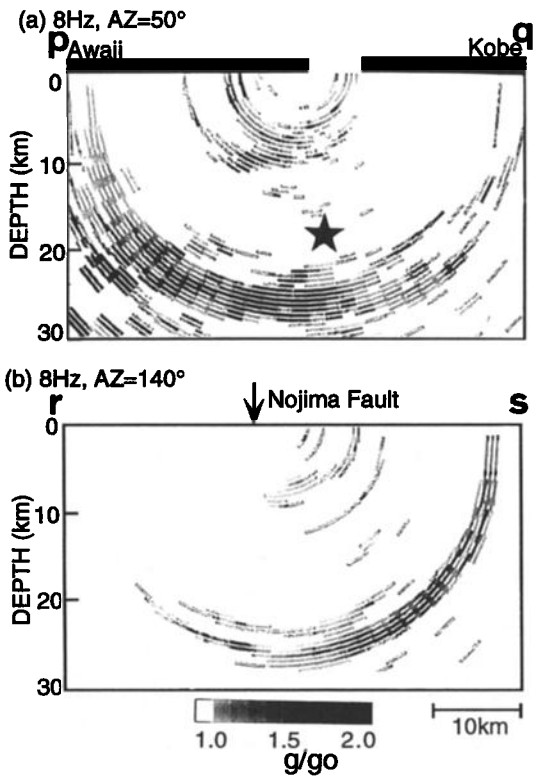

Figure 5. Vertical cross sections of P wave scatterer distribution. (a) and (b) are those along the lines (a) N50E and (b) N140E shown in Fig. 1, respectively. Scattering strength ratio is shown by the scale at the bottom. Dark portion shows high ratio of scattering strength to the background scattering coefficient (g/g_0).

P-wave Scatterer Distribution

Obtained images by stacking for the 12 shots are shown in Figs. 5(a) and 5(b). These figures show vertical cross-sections of the scattering strength distribution along the lines parallel (N50E) and perpendicular (N140E) to the fault plane. In Fig. 5(a), we can see some areas having relatively high scattering strength. Scatterers with high scattering strengths are clustered at depths of about 5-10km to the southwest of the array. High strength scatterers are also distributed at depths of 20 - 25km. The deeper one spreads over 30km horizontally from northeast to southwest beneath the array. This part corresponds to clear phases found in Fig. 2 at a lapse time between 8 to 14 sec. The star symbol denotes the hypocenter of the 1995 Hyogo-ken Nanbu Earthquake. It seems that the scattering strength is relatively strong just below the hypocenter. This indicates that the earthquake initiated at an inhomogeneous zone with a short wave length of several hundreds meters, since the wavelength of inhomogeneity detected in this analysis is about 500m. In general, strong scatterers are distributed in the southwestern part of the target area where many active faults are located (e.g., Nojima fault along which the rupture of the earthquake appeared at the surface). We also find other regions with high scattering strengths at depths of about 10km and 20km in Fig. 5(b). These regions are slightly shifted to southeast from the fault plane. No other areas having remarkable scattering strengths are found.

Zhao et al. [1996] estimated the P and S wave velocity structure of the crust in this region by using travel time tomographic technique. They concluded that a low velocity and high Poisson's ratio zone of about 300km^2 exists at and around the hypocenter. They interpreted that this zone is composed of fractured rocks filled with water. This zone with a high Poisson's ratio around the hypocenter partially corresponds to that with a high scattering strength. This may supports the inference by *Zhao et al.* [1996] that the earthquake initiated at the fractured area. A similar spatial relation between the scattering strength, seismic velocity and Poisson's ratio can be found in the vertical cross-section along the line of N140E.

The rupture process of the 1995 Hyogo-ken Nanbu Earthquake has been studied by many researchers and is reviewed by *Takemura* [1996]. Most of these studies are based on longer period seismic waves (< 1Hz) than the present case and/or on geodetic data. *Kakehi et al.* [1996] estimated the location of the areas radiating high frequency (2 - 10Hz) seismic waves along the fault plane of the earthquake by inverting envelopes of acceleration seismograms. Their obtained result shows that high frequency waves are radiated from the area beneath Awaji Island. We see again a close spatial relationship between the high scattering strength zone and zone of the high frequency radiation beneath Awaji Island. Since the frequency range of the present study is similar to that of *Kakehi et al.* [1996], this close relationship suggests that the inhomogeneity generating distinct scattering waves affects the earthquake faulting process, such as barriers.

Conclusion

We developed a method to estimate scattering strength distribution combining slant stacking and diffraction curve summation processing. We applied this method to the seismic array data deployed in the northern part of Awaji Island, close to the hypocenter of the 1995 Hyogo-ken Nanbu Earthquake. 12 shots of explosions by R.G.E.S were observed by the array. After band-pass filtering in a range from 6 to 10Hz, the waveforms of the explosions are slant stacked into directions of scattered waves coming to the array. AGC and diffraction curve summation processing is applied to the stacked waveforms to estimate a spatial distribution of P wave scattering strength in this frequency band. The obtained scatterer distribution shows high scattering strength is distributed around the hypocenter and in the southwestern part of the fault plane of the 1995 Hyogo-ken Nanbu Earthquake. This distribution partially correlates in space with seismic velocity structure and the rupture process of the earthquake.

Acknowledgments.

We appreciate the R.G.E.S for permitting us to use of their explosions. The authors also thank researchers of Tohoku, Hirosaki and Yamagata Universities and National Research Institute for Earth Science and Disaster Prevention for the array observation. Critical reviews and comments by two anonymous reviewers helped to improve this manuscript. This research was partially supported by the Grant-in-Aid for Scientific Research No. 09740347 from the Ministry of Education, Science, Sports and Culture of Japan.

References

Hirata, N., S. Ohmi, S. Sakai, K. Katsumata, S. Matsumoto, T. Takanami, A. Yamamoto, T. Iidaka, T. Urabe, M. Sekine, T. Ooida, F. Yamazaki, H. Katao, Y. Umeda, M. Nakamura, N. Seto, T. Matsushima, H. Shimizu, and Japanese University Group of the Urgent Joint Observation for the 1995 Hyogo-ken Nanbu Earthquake, Urgent joint observation of aftershocks of the 1995 Hyogo-ken Nanbu Earthquake, *J. Phys. Earth*, *44*, 4, 317-328, 1996.

Ide, S., M. Takeo, and Y. Yoshida, Source process of 1995 Kobe earthquake: determination of spatiotemporal slip distribution by Bayesian modeling, *Bull. Sismol. Soc. Am.*, *86*, 547-566, 1996

Kakehi, Y., K. Irikura, and M. Hoshiba, Estimation of high-frequency wave radiation areas on the fault plane of the 1995 Hyogo-ken Nanbu Earthquake by the envelope inversion of acceleration seismograms, *J. Phys. Earth*, *44*, 5, 505-518, 1996.

Nishigami, K., A new inversion method of coda waveforms to determine spatial distribution of coda scatterers in the crust and uppermost mantle, *Geophys. Res. Lett.*, *18*, 12, 2225-2228, 1991.

Research Group for Explosion Seismology, Intensive seismic refraction experiment in and around the source region of the 1995 southern Hyogo Prefectural earthquake, *Abstract Japan Earth Planet. Sci. Joint Met.*, 38, 1996.

Revenaugh, J., A scattered-wave image of subduction beneath the transverse range, *Science*, *268*, 1888-1892, 1995.

Takemura, M., Review of source process studies for the 1995 Hyogo-ken-Nanbu earthquake Part.1 Results from waveform Inversion, *Prog. and Abs. Seismol. Soc. Japan*, *2*, A49, 1996.

Yoshida, S., K. Koketsu, B. Shibazaki, T. Sagiya, T. Kato, and Y. Yoshida, Joint inversion of near- and far-field waveform and geodetic data for the rupture process of the 1995 Kobe Earthquake, *J. Phys. Earth*, *44*, 5, 437-454, 1996.

Zhao, D., H. Kanamori, H. Negishi, and D. Wiens, Tomography of the source area of the 1995 Kobe Earthquake: evidence for fluids at the hypocenter?, *Science*, *274*, 1891-1894, 1996.

S. Matsumoto, Institute of Applied Earth Science, Mining College, Akita University, Akita 010, Japan. (e-mail: matumoto@ipc.akita-u.ac.jp)

K. Obara, National Research Institute for Earth Science and Disaster Prevension, Tsukuba 305, Japan. (e-mail: obara@bosai.go.jp)

A. Hasegawa, Research Center for Prediction of Earthquakes and Volcanic Eruptions, Faculty of Science, Tohoku University, Sendai 980, Japan. (e-mail: hasegawa@aob.geophys.tohoku.ac.jp)

(Received: September 3, 1997; Revised: March 10, 1998; Accepted: March 17, 1998)